Egyptian Journal of Chemistry
http://ejchem.journals.ekb.eg/

Adsorption Studies on Chromium Ion Removal from Aqueous Solution Using Magnetite Nanoparticles

S. M. Abobakr[1] and N. I. Abdo*[2]
[1]*Higher Institute of Engineering and Technology, New Damietta, Egypt*
[2]*Higher Institute of Engineering and Technology, New Borg Al Arab, Alexandria, Egypt*

Abstract

The existence of toxic metals in surface and waters, even at hint levels, poses a considerable danger to humans and the ecosystem. So, removal of heavy metals is an important process. In this study, an adsorbent made of magnetite nanoparticles (MNPs) was employed to remove chromium ions form aqueous solution. MNPs (before and after) were characterized by SEM, FT-IR and XRD techniques. These nanoparticles have a spherical shape and their diameter about 11 nm. A number of factors were studied including (concentration, pH, time, sorbent dose and temperature). Thermodynamics, kinetics and adsorption isotherms of MNPs were all investigated. This adsorption describes as a spontaneous process, endothermic and pseudo-second order kinetics. The adsorption isotherm was described by the Temkin model.

Keywords: Magnetite nanoparticles (MNPs), Chromium (VI), SEM, FT-IR, XRD, Adsorption mechanisms, Temkin isotherm

1. Introduction

Industrial wastewater is oftentimes characterized by considerable heavy metal content and therefore treatment is required to disposal so as to avoid water pollution. Heavy metals are released from industries such as metal plating, batteries, mining, etc. [1].

Trivalent and hexavalent chromium are the common existing oxidation states of chromium. Public attentions over chromium are mostly related to Cr (VI) due to its high toxic ability for ecosystem [2]. Hexavalent chromium usually exists in wastewater as oxyanions such as chromate (CrO_4^{2-}) and bichromate ($Cr_2O_7^{2-}$) and dose not precipitate using traditional precipitation methods [3].

Mostly favourable technique for removal of heavy metals from industrial wastewaters, adsorption technology has been utilized for several years and the efficacy of different adsorbents has been established [4-12].

The usage of magnetic adsorbent technology to solve environmental issues has received significant attention in recent years. Magnetic adsorbent can be used to adsorb contaminants from aqueous or gaseous effluents. After ion adsorption, the adsorbent can be discrete from the medium by a simple magnetic process [13-18].

MNPs have attracted concern in many environmental engineering applications. With sizes ranging from 1 to 100 nm, high surface ratio, and high loading capacity, MNPs were used as good adsorptive substances for contaminants [19-21].

The current study aimed to prepare MNPs by co-precipitation method and then used as an adsorbent for removal of Cr (VI) from aqueous solution. The effects of variables influencing the removal process, adsorption kinetics and isotherms for Cr (VI) onto MNPs were evaluated

Materials and Methods

Materials

Potassium bichromate ($K_2Cr_2O_7$), ferric chloride ($FeCl_3.6H_2O$), ferrous sulfate ($FeSO_4.7H_2O$), ammonium hydroxide (NH_4OH), dilute hydrochloric acid (HCl), dilute sulfuric acid (H_2SO_4) and dilute sodium hydroxide (NaOH) were used for this study. A stock standard solution of potassium bichromate at a concentration of 500 mg l^{-1} was prepared in DH_2O. Stock solutions with the concentration of 10, 25 and

*Corresponding author e-mail: nabiha_ibrhim@yahoo.com.
Receive Date: 10 September 2021, Revise Date: 26 December 2021, Accept Date: 03 January 2022
DOI: 10.21608/ejchem.2022.95319.4475

50 mg l^{-1} of $K_2Cr_2O_7$ were prepared.

Preparation of magnetite nanoparticles (MNPs)

MNPs were synthesized by co-precipitation method as reported previously [18]. Magnetite nanoparticles (MNPs) were synthesized by chemical coprecipitation of Fe^{2+} (1 mol) and Fe^{3+} (2 mol) with the addition of NH_4OH (33 wt%).

Batch Experimental

The Cr (VI) was made up in stock solution of concentration (2.825 g of Cr in 1000 ml of DH_2O) and was subsequently diluted to the required concentrations from 10 to 100 mg l^{-1}. The effect of some parameters such as pH (3-9) and adsorbent dosage (0.04–0.2 g) was made by known amount of MNPs and 25 ml of Cr solution. The sorption studies were performed at different temperatures (25 ºC–95 ºC). The mixture was shaken using water bath at 240 rpm (25 °C for 30 min). In all these different parameters, the amount of chromium taken by adsorbent is calculated as:

$$q_e = (C_i - C_e)\, v/m \quad (1)$$

Where: (q_e; the amount of Cr taken by adsorbent (mg/g)), (C_i and C_e; the concentrations of Cr at initial and equilibrium (mg l^{-1}), respectively), (v; the volume of solution (l)) and (m; the mass of adsorbent (g)). Also the removal efficiency is calculated as:

$$\%\text{Removal of Cr (VI)} = (C_i - C_f)/C_i * 100 \quad (2)$$

Where: (C_i and C_f the initial and final Cr concentrations (mg l^{-1}), respectively).

Characterization

FT-IR was carried out using (FT/IR-4100) spectrophotometer (ThermoFisher Nicolet IS10, USA) in KBr pellets at room temperature. Micrographs of the samples were taken using SEM (JSM-6510, JEOL, Ltd.). XRD measurements were recorded on (Shimadzu LabX XRD-6000). UV-visible spectroscopic analysis was carried out on Oasis Scientific (PG Instruments T80). The pH of solutions was adjusted with a Hanna model 211-pH meter.

Results and Discussion

Morphology Characterization

The morphology and particle size of the prepared MNPs as a spherical shape with about 11 nm were investigated by TEM in our previously prepared magnetite nanoparticles [18].

The morphology of MNPs before adsorption with spherical and aggregated porous surface was investigated previously by SEM (figure 1a) [18]. The micrograph of MNPs-Cr (figure 1b) displayed a surface with slightly granular particles in a smooth layer on the magnetite surface, which indicated coagulation of the toxic metals onto the MNPs.

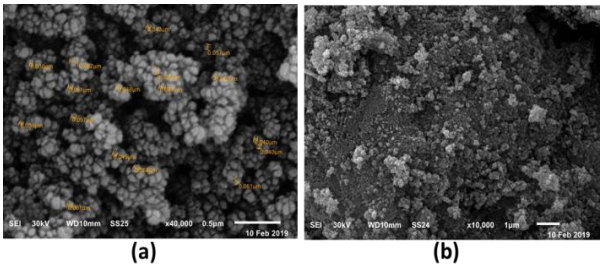

Figure 1. SEM micrographs: (a) MNPs; (b) MNPs-Cr (VI).

The FT-IR spectra of synthesized MNPs before adsorption with the characteristic bands for MNPs were previously investigated (figure 2a) [18].

The disappearance and shift of the bands attributed to the vibration modes of Fe-O around range from 404 cm^{-1} to 634 cm^{-1} (figure 2b) indicated the participation of the oxygen of these groups in an interaction to the metal ions of Cr (VI). The observed shift to higher and/or to lower wavelength or disappearance of bands is a good indication for the adsorption process.

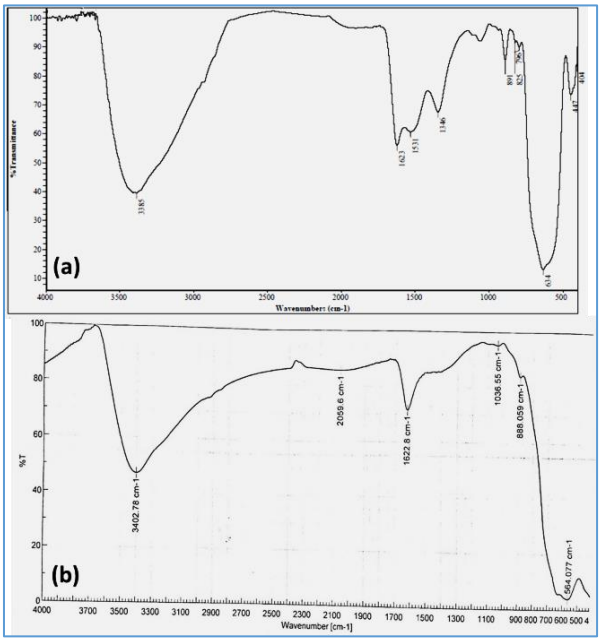

Figure 2. FT-IR spectra: (a) MNPs; (b) MNPs-Cr (VI).

Figure 3a, shows the XRD patterns for MNPs. A series of characteristic peaks observed at 2θ = 35.78°, 41.82°, 50.84°, 57.5°, and 62.82°, which corresponds to (110), (113), (024), (018) and (300). The crystalline size of MNPs was calculated at approximately 11 nm with Scherrer equation [22].

As shown in figure 3b, there is a visual difference in the patterns with respect to shifting, decrease in intensity and disappearance of peaks which gives an indication of the adsorption process. This in turn contributed to the loss of crystallinity of MNPs due to adsorption of chromium.

Adsorption Studies

Effect of Cr (VI) concentration

The effect of Cr (VI) concentration with using MNPs were studied through several Cr (VI) concentrations with optimum 0.2 g adsorbent dosage at ambient temperature (25ºC) for 30 min equilibrium time (figure 4). The %removal decreased from 96.1% to 87.2% with the increased in Cr (VI) concentration from 40 to 100 ppm. The initially rapid adsorption is attributed to the presence of an efficient area on the MNPs and with the slow taking of these areas the adsorption becomes less efficient due to the available adsorption sites are restricted. The equilibrium Cr (VI) concentration isobserved to be 40-50 ppm at which the maximum percentage Cr (VI) adsorbed (removal efficiency 96.058%) was obtained.

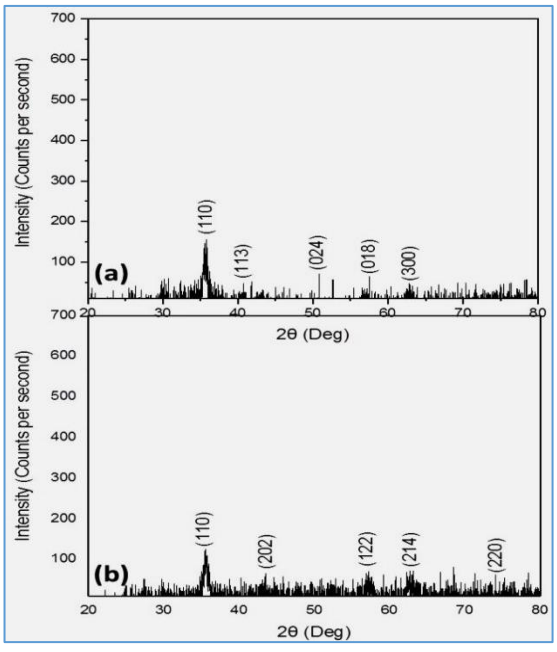

Figure 3. XRD patterns: (a) MNPs; (b) MNPs-Cr (VI).

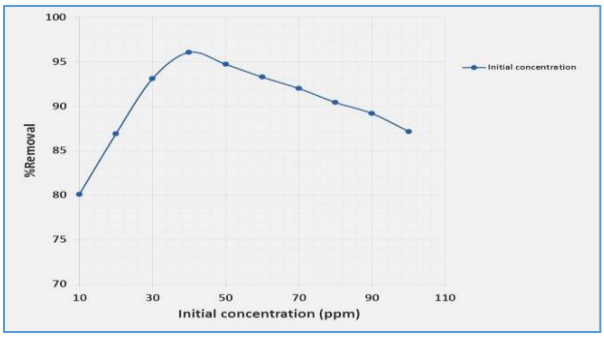

Figure 4. Influence of initial concentration of Cr (VI) on the adsorption process.

Effect of pH

The removal efficiency was found to be pH-dependent, as the removal efficiency decreased from 69.9% to 39.1%; 87.1% to 41.9% and 90.9% to 46.5% for 50, 25 and 10 ppm initial Cr (VI) concentrations when the pH increased from 3 to 9 (figure 5). At a lower pH, Cr (VI) exist mainly is CrO_4^{2-} and $Cr_2O_7^{2-}$ [3], which possess negative charges, while the surface of MNPs is charged positively. Therefore, at lower pH, $Cr_2O_7^{2-}$ and CrO_4^{2-} were adsorbed onto the MNPs surface, resulting in a high adsorption (the best uptake at pH = 3).

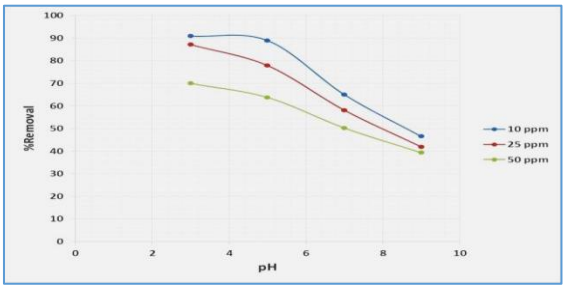

Figure 5. Influence of pH on the adsorption process.

Effect of contact time

The removal rate (%) increases with time and detects a fast removal during the first few minutes of contact until the equilibrium state is reached in a short time (35 min at 25 ºC). The maximum percentage of Cr (VI) adsorbed onto MNPs (removal efficiency 98.5%, 94.4% and 86.6%) for the different initial concentrations of Cr (VI) 10, 25 and 50 ppm, respectively was obtained (figure 6).

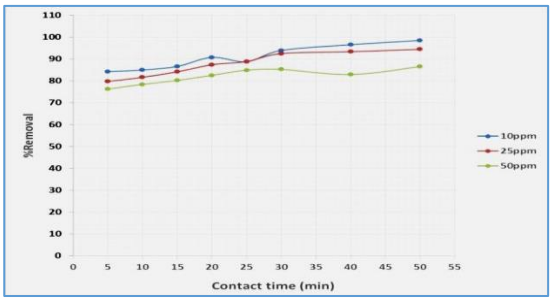

Figure 6. Influence of contact time on the adsorption process.

Effect of sorbent dose

It was found that the %removal (93.9%, 86.6% and 74.4%) of different concentrations 10, 25 and 50 ppm of Cr (VI) adsorbed was obtained at dosage of 0.2 g of MNPs (figure 7). Increasing the dosage of MNPs from 0.04 g to 0.2 g produces increase in %removal of Cr (VI). Any further increases in the adsorbent dose after 0.2 g lead up to desorption due to agglomeration of particles.

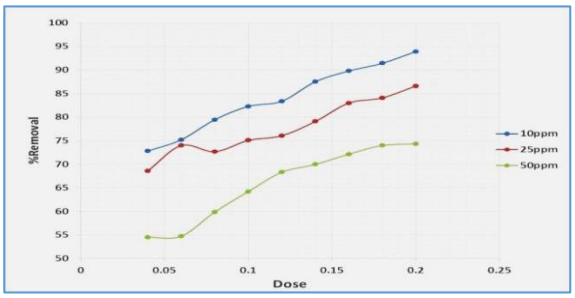

Figure 7. Influence of sorbent dose (MNPs) on the adsorption process.

Effect of temperature

The rate of Cr (VI) uptake increased with an increase in temperature from 62.9% to 80.7%; 66.4% to 89.9% and 71.7% to 97.5% at 25 °C to 95 °C with 0.2 g of MNPs in 30 min from 50, 25 and 10 ppm Cr (VI) solution, indicating that the process is endothermic (figure 8). This may be due to a result of increasing adsorption capacity [23].

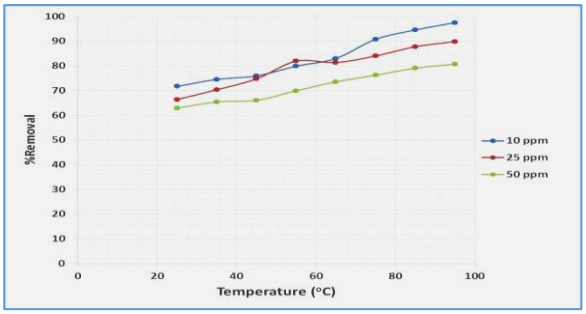

Figure 8. Influence of temperature on the adsorption process.

Adsorption isotherms

Langmuir isotherm

Langmuir equation used is given below [24]:

$$q_e = (q_m\, b\, C_e) / (1+b\, C_e) \quad (3)$$

Where: (C_e; equilibrium concentration of Cr), (q_e; the amount of Cr adsorbed at equilibrium), (q_m; Langmuir monolayer adsorption capacity (mg/g)), and (b; Langmuir constant (l/mg)). The equation is linearized by different ways to give the next equation:

$$C_e/q_e = 1/(q_m b) + C_e/q_m \quad (4)$$

The straight-line plot of C_e/q_e vs. C_e is shown in figure 9. The slope and the intercept of the plot gave the values of q_m and b at 23.74 and 0.069 for Cr (VI).

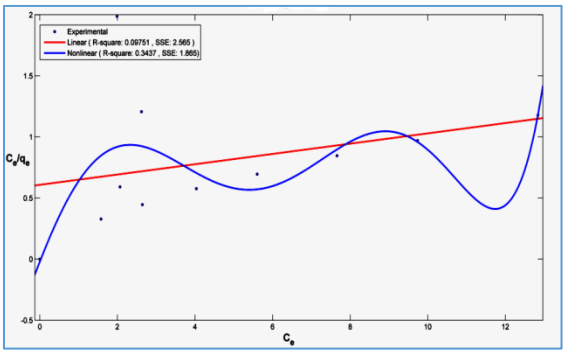

Figure 9. Langmuir adsorption isotherm.

Freundlich isotherm

It is often used to depict non-specific adsorption that comprises of heterogeneous surfaces [25].

$$q_e = K_f * C_e^{\,1/n} \quad (5)$$

The equation is linearized by different ways to give the next equation:

$$ln\ qe = ln\ K_f + (1/n)\ ln\ C_e \quad (6)$$

Where: (f; Freundlich coefficients (l/g)) and (n; related to adsorption intensity) were obtained from the slope and the intercept of the linearized Freundlich plots. The plot of ln C_e versus *ln* q_e of Cr (VI) in figure 10 is straight line over the entire concentrations of Cr (VI). The values of K_f and 1/n computed from the intercept and slope of the plot were equal to 1.452 and 0.885 for Cr (VI).The amount of 1/n < 1 indicates that the sorption strength is slightly miniature at lower equilibrium concentration [26, 27].

Temkin isotherm

It assumes that the heat of adsorption of all the molecules in the layer decreases linearly with coverage due to adsorbate species adsorbent interactions [28, 29], and adsorption is described by a

regular distribution of binding energies, up to some maximum binding energy [30].

$$q_e = q_m \ln (t + C_e) \quad (7)$$

The equation is linearized by different ways to give the next equation:

$$q_e = q_m \ln t + q_m \ln C_e \quad (8)$$

Where: (q_e; the concentration of Cr removed (mg/g)), (t; the equilibrium binding constant (l/g)) and (q_m; constant related to heat of adsorption (J/mol).

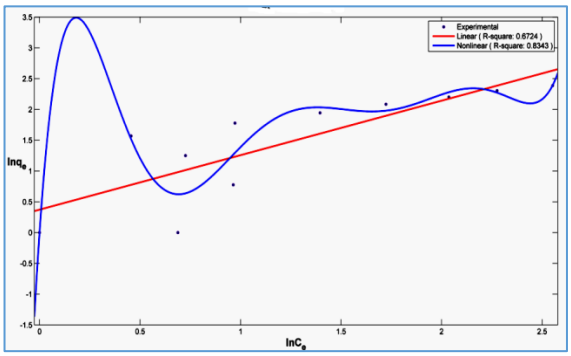

Figure 10. Freundlich adsorption isotherm.

The linear plot of q_e versus ln C_e for both the adsorption system gave good fit for the Temkin isotherm as shown in figure 11. The values of q_m and t from the slope and intercept were equal 4.229 and 1.092 for Cr (VI), respectively.

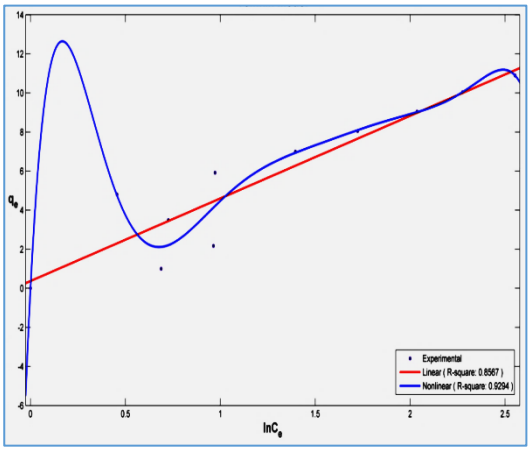

Figure 11. Temkin adsorption isotherm.

Dubinin-Radushkevich isotherm (D-R)

It is used to evaluate the characteristic porosity of the adsorbent and the apparent energy of adsorption onto a heterogeneous surface [31, 32]. It is illustrated by the equation:

$$q_e = q_m e^{(-D\mathcal{E}2)} \quad (9)$$

The equation is linearized by different ways to give the next equation:

$$Ln\ q_e = ln\ q_m - D\mathcal{E}^2 \quad (10)$$

$$\mathcal{E} = RT\ ln\ (1+1/C_e) \quad (11)$$

Where: (q_e; amount of Cr adsorbed on MNPs), (q_m; D-R isotherm constant mg/g)), (D; activity coefficient), (C_e; equilibrium concentration of Cr in mg/l) and (ε; RT ln (1+1/C_e)).

A plot of ln q_e versus ε^2 as shown in figure 12 yielding straight line confirms the model. The D-R constant can be specified from the intercept of the straight-line diagram. The values of q_m and D from the intercept and slopeof the plot, were equal to 5.911 and 0.603 for Cr (VI).

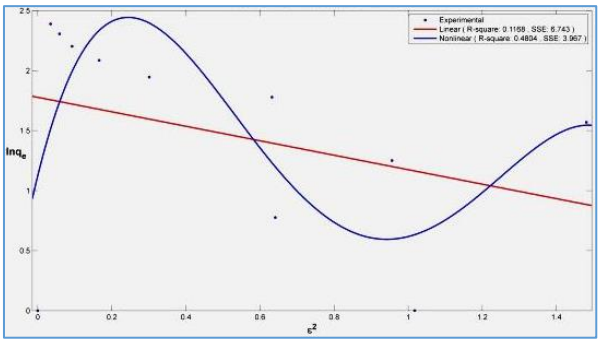

Figure 12. Dubinin-Radushkevich adsorption isotherm.

The isotherm parameters determined by linearization and the nonlinear regression of the Langmuir, Freundlich, Temkin and Dubinin equations, using Standard Error of the Estimate function (SEE), together with the correlation coefficient (R^2) and error values, are summarized in Table 1. It was found that the regression methods revealed that Cr (VI) adsorption were better fitted to the Temkin isotherm in terms of the R^2, because of the higher R^2 values than those of other models.

Adsorption Kinetics

The dynamics of the adsorption of Cr (VI) onto MNPs were inspected using the Lagergren's pseudo-first order (Eq. 12) and pseudo-second order (Eq. 13) equations:

$$\text{Log } (q_e\text{-}q_t) = \text{Log } q_e - k_1 t / 2.303 \quad (12)$$

$$t / q = 1/ K_2 q_e^2 - [1 / q_e] t \quad (13)$$

where q_e and q_t are the amount of Cr (VI) adsorbed per unit mass at equilibrium and at any time (t), k_1 is the first-order adsorption rate constant (1/min), k_2 is the pseudo-second order rate constant (g/mg. min). The K_1 and K_2 have been calculated from the intercept of the corresponding of log (q_e-q_t) versus t as shownin figure 13 and t/q versus t shown in figure 14, and are

tabulated in Table 2 along with correlation coefficients values. According to the correlation coefficient value (R^2), it was confirmed that the adsorption system followed the pseudo-second order rate equation.

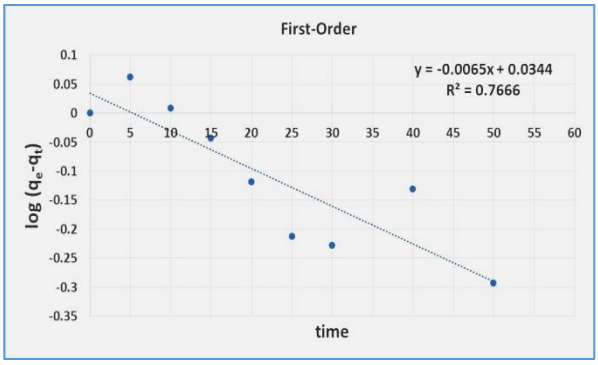

Figure 13. Pseudo-first order adsorption kinetics of Cr (VI) onto MNPs.

Figure 14. Pseudo-second order adsorption kinetics of Cr (VI) onto MNPs.

Thermodynamic studies

Thermodynamic equations can be expressed as follow:

$$\Delta G = - RT \ln K \quad (14)$$

$$K = q_e/C_e \quad (15)$$

$$\Delta G = \Delta H - T\Delta S \quad (16)$$

Where: (ΔG; the Gibbs free energy (KJ /mol)), (ΔH; the change in enthalpy (KJ/mol)), (ΔS; the entropy change (KJ/mol K)), (T; the absolute temperature in (K)), (K; the equilibrium constant (1/q)), (R; the universal gas constant (KJ /mol K)), (q_e; the amount of adsorbed Cr (VI) onto MNPs (mg/ g)), and (C_e; the equilibrium concentration of Cr (VI) in the solution (mg l^{-1})).

The ΔH° and ΔS° have been calculated from the intercept of the corresponding of ln (q_e/C_e) versus 1/T as shown in figure 15 and were found to be 12365.171 J/mol and 27.948435 J/mol.K, respectively. We calculate ΔG° (ΔG° = ΔH°- TΔS°) as listed in Table 3 and shown in figure 16.

The decrease in the value of ΔG° with an increase in temperature indicates that the adsorption process of Cr (VI) on MNPs becomes more favorable at higher temperatures. We found that at high temperature, ΔH, ΔS and ΔG have positive value so; the process is spontaneous at high temperatures (endothermic process). The positive amount of ΔS displays the increased disorder at the solution interface through the adsorption of Cr (VI) on the adsorbent [33, 34].

Table 1. Constants and correlation coefficients for the four isotherms.

Model	Parameter	Linear regression	Nonlinear regression
Langmuir	q_m (mg/g)	23.74	
	b (l/mg)	0.069	
	R^2	0.0975	0.3437
	SEE	2.565	1.865
Frundlich	K_f (mg/g)	1.452	
	1/n	0.885	
	R^2	0.6724	0.8343
	SEE	2.501	1.265
Temkin	q_m (mg/g)	4.229	
	t (1/g)	1.092	
	R^2	0.8567	0.9294
	SEE	19.652	9.662
Dubinin (D-R)	D (mol^2/J^2)	0.603	
	q_m (mol/g)	5.911	
	R^2	0.1168	0.4804
	SEE	6.743	3.967

Table 2. Adsorption dynamic constants (calculated and experimental q_e values obtained at 50 ppm of Cr (VI).

C_i (ppm)	q_e Exp. (mg/g)	Pseudo-first order kinetic model			Pseudo-second order kinetic model		
		K_1 (1/min)	q_e Cal. (mg/g)	R^2	K_2 (g/mg min)	q_e Cal. (mg/g)	R^2
50	5.9196	0.015	1.0824	0.7666	0.2831	5.2897	0.9988

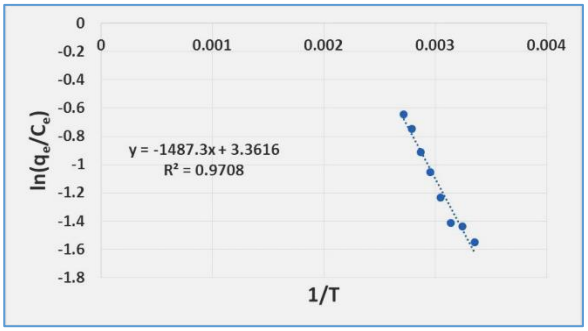

Figure 15. Linear plot of ln q_e/C_e versus 1/T.

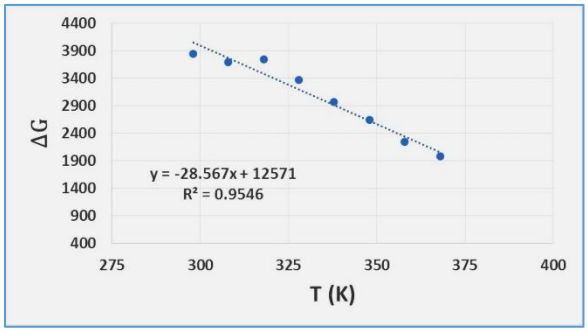

Figure 16. Plot of ΔG° versus T.

Table 3. Calculation of ΔG° at different temperatures.

t (°C)	T (K)	ΔG
25	298	4036.5
35	308	3757.1
45	318	3477.6
55	328	3198.1
65	338	2918.6
75	348	2639.1
85	358	2359.6
95	368	2080.1

Conclusion

MNPs were synthesized using co-precipitation method. MNPs structure was confirmed using SEM, FT-IR and XRD. The adsorption of Cr (VI) was found to increase with increase in time, increase temperature, decrease metal concentration and decrease pH up to equilibrium amount. A pseudo-second order equation well explained the kinetic data and revealed the physisorption. Moreover, the equilibrium data were described by Temkin model.

Conflicts of interest

There are no conflicts to declare

References

1. Achanai, B., Nattawut, C., Kessarin, T., Supparoek, J., Sutheera, P., Removal of Cu^{2+} from aqueous solution by biosorption rice-straw- an agricultural waste biomass. *International Journal of Environmental Science and Development*, 3(1), 10-14 (2012).
2. Weng, C-H., Sharma, Y.C. and Chu, S-H., Adsorption of Cr (VI) from aqueous solutions by spent activated clay. *Journal of Hazardous Materials*, 155, 65-75 (2008).
3. Hu, J., Chen, G., Lo, I.M.C., Removal and recovery of Cr (VI) from wastewater by maghemite nanoparticles. *Water Research*, 39(18), 4528-4536 (2005).
4. Lazaridis, N.K. and Asouhidou, D.D., Kinetics of sorptive removal of chromium (VI) from aqueous solutions by calcined Mg-Al-CO_3 hydrotalcite**,** *Water Res*earch, 37(12), 2875-2882 (2003).
5. Younas, F., Mustafa, A., Farooqi, Z.U.R., Wang, X., Younas, S., Mohy-Ud-Din, W., Hameed, M.A., Abrar, M.M., Maitlo, A.A., Noreen, S. and Hussain, M.M., Current and emerging adsorbents technologies for wastewater treatment: trends, limitations, and environmental implications. *Water*, 13, 215-239 (2021).
6. Hur, J., Shin, J., Yoo, J. and Seo, Y.S., Competitive adsorption of metals onto magnetic graphene oxide: comparison with other carbonaceous

adsorbents. *The Scientific World Journal*, 2015 (2015). id. 836287
7. Sengupta, S. and Mondal, R., A novel gel-based approach to wastewater treatment-unique one-shot solution to potentially toxic metal and dye removal problems. *Journal of Materials Chemistry A: Materials for Energy and Sustainability*, 2, 16373–16377 (2014).
8. Fu, F.L. and Wang, Q., Removal of heavy metal ions from wastewaters: A review. *Journal of Environmental Management*, 92, 407–418 (2011).
9. Zhang, X, Liu, H., Yang, J., Zhang, L., Cao, B., Liu, L. and Gong, W., Removal of cadmium and lead from aqueous solutions using iron phosphate-modified pollen microspheres as adsorbents. *Reviews on Advanced Materials Science*, 60, 365–376 (2021).
10. Spurthi, L., Chandrika, K., Kausalya, C.L., Yashas,S., Brahmaiah, T., Prasad, K.S.S., Removal of chromium from wastewater using low cost adsorbent. *World Journal of Pharmacy and Pharmaceutical Sciences*, 4(10), 2164-2173 (2015).
11. Yohanis, B., Seyoum, L., Getachew, A., Removal of chromium from synthetic wastewater by adsorption onto Ethiopian low-cost odaracha adsorbent. *Applied Water Science*, 10, 227-237 (2020).
12. Dessalew, B., Removal of chromium from industrial wastewater by adsorption using coffee husk. *Journal of Materials sciences & Engineering*, 6(2), 1000331 (2017).
13. Oliveira, L.C.A., Rios, R.V.R.A., Fabris, J.D., Sapag, K. and Lago, R.M., Clay-iron oxide magnetic composites for the adsorption of contaminants in water. *Appl. Clay Sci*., 22,169-177 (2003).
14. Ahmad, I., Siddiqu, W.A. and Ahmad, T., Synthesis and characterization of molecularly imprinted magnetite nanomaterials as a novel adsorbent for the removal of heavy metals from aqueous solution. *Journal of Materials Research and Technology*, 8(5), 4239-4252 (2019).
15. Hossain, M.T., Hossain, M.M., Begum, M.H.A., Shahjhan, M. and Islam, M.M., Magnetite (Fe_3O_4) nanoparticles for chromium removal. *Bangladesh Journal of Science and Industrial Research*, 53(3), 219-224 (2018).
16. Zhang, J., Linn, S., Han, M., Su, Q., Xia, L. and Hui, Z., Adsorption Properties of Magnetic Magnetite Nanoparticle for Coexistent Cr (VI) and Cu (II) in Mixed Solution. *Water*, 12, 446-458 (2020).
17. Stoian, O., Covaliu, C.I., Paraschiv, G., Catrina, G., Nita-Lazar, M., Matei, E., Biris, S.S. and Tudor, P., Magnetite Nanomaterial used for lead ions removal from industrial wastewater, *Materials*, 14, 2831-2841 (2021).
18. Abobakr, S.M., Abdo, N.I., Mansour, R.A., Remediation of Contaminated Water with Crystal Violet dye by using magnetite nanoparticles: synthesis, characterization and adsorption mechanism studies. *Journal of Environmental Studies*, 6, 1-10 (2020).
19. Kong, L., Gan, X., Ahmad, A.L.b., Hamed, B.H., Evarts, E.R., Ooi, B. And Lim, J., Design and synthesis of magnetic nanoparticles augmented microcapsule with catalytic and magnetic bifuntionalities for dye removal. *Chemical Engineering Journal*, 197, 350–358 ((2012).
20. Lotfi Zadeh Zhad, H.R., Aboufazeli, F., Sadeghi, O., Amani, V., Najafi, E. And Tavassoli, N., Tris(2-aminoethyl)amine-functionalized F_3O_4 magnetic nanoparticles as a selective sorbent for separation of silver and gold ions in diffrent pHs. *Journal of Chemistry*. 2013, (2013).
21. Simona, G.M., Maria, A.N., Eliza, M., Anamaria, T., Robert, I. And Cornelia, P., Removal of colored organic pollutants from wastewaters by magnetite/nanocomposite: single and binary systems. *Journal of Chemistry*, 2018 (2018).
22. Ashraf, R., Bashir, M., Raza, M.A., Riaz, S. and Naseem, S., Effect of calcination on structural and magnetic properties of Co doped ZnO nanostructures. *IEEE Transactions on Magnetics*, 51, 1–4 (2015).
23. Gad, H.M.H., El-Sayed, A., Activated carbon from agricultural by-products for the removal of Rhodamine-B from aqueous solution. *Journal of Hazardous Materials*, 168, 1070-1081 (2009).
24. Hall, K.R., Eagleton, L.C., Acrivos, A. and Vermeulen, T., Pore and solid diffusion kinetics n fixed bed adsorption under constant pattern conditions. *Industrial & Engineering Chem*istry *Fundamentals*, 5(2), 212–223 (1966).
25. Hutson, N.D. and Yang, R.T., Theoretical basis for the Dubinin-Radushkevitch (D-R) adsorption isotherm equation. *Adsorption*, 3(3), 189-195 (2000).
26. Farag, A.B., Soliman, M.H., Abdel-Rasoul, O.S., El-Shahawi, M.S., Sorption characteristics and chromatographic separation of gold (I and II) from silver and base metal ions using polyurethane foams. *Analytica Chimica Acta*, 601, 218–229 (2007).
27. Al-Ahmary K.M., Retention profile of cadmium and lead ions from aqueous solutions onto some selected local solid sorbents. *Journal of Taibah University for Science*, 2, 52-61 (2009).
28. Temkin, M. and Pyzhev, V., Kinetics of ammonia synthesis on promoted iron catalysts. *Acta Physicohimica U.R.S.S.*, 12, 327–356 (1940).
29. Aharoni, C., Ungarish, M., Kinetics of activated chemisorption. Part 2: Theoretical models,

Journal of the Chemical Society, Faraday Transactions, 73 456–464 (1977).

30. Wang, H., Su, J.Q., Zheng, X.W., Tian, Y., Xiong, X.J. and Zheng, T.L., Bacterial decolorization and degradation of the reative dye red 180 by Citrobacter sp. CK3. *International Biodeterioration and Biodegradation*, 63, 395-399 (2009).
31. Gunay, A., Arslankaya, E. and Tosun, I., Lead removal from aqueous solution by natural and pretreated clinoptilolite: Adsorption equilibrium and kinetics. *Journal of Hazardous Mater*ials, 146, 362–371 (2007).
32. Dabrowski,, A., Adsorption — from theory to practice. *Advances in Colloid and Interface Sci*ence, 93, 135–224 (2001).
33. Paska, O.M., Pacurariu, C. and Munteon, S.G., Kinetic and thermodynamic studies of methylene blue biosorption using corn-husk. *RSC Advances*, 4, 62621-62630 (2014).
34. Anusha, S., Azrina, A., Pichiah, S. and Manickam, M., Adsorption of mercury (II) ion from aqueous solution using low-cost activated carbon prepared from mango kernel. *Asia-Pacific Journal of Chemical Engineering*, 8, 1-10 (2012).